Biomaterials 83 (2016) 23–36

Contents lists available at ScienceDirect

Biomaterials

journal homepage: www.elsevier.com/locate/biomaterials

Injectable hydrogel promotes early survival of induced pluripotent stem cell-derived oligodendrocytes and attenuates longterm teratoma formation in a spinal cord injury model

T. Führmann [a, b], R.Y. Tam [a, b], B. Ballarin [b], B. Coles [c, d], I. Elliott Donaghue [a, b], D. van der Kooy [c], A. Nagy [e], C.H. Tator [f], C.M. Morshead [b, g], M.S. Shoichet [a, b, *]

[a] Department of Chemical Engineering and Applied Chemistry, University of Toronto, 200 College Street, Toronto, Ontario, Canada M5S 3E5
[b] Institute of Biomaterials and Biomedical Engineering, 160 College Street, Room 530, Toronto, Ontario, Canada M5S 3E1
[c] Department of Molecular Genetics, University of Toronto, 1 King's College Circle, Toronto, Ontario M5S 1A8, Canada
[d] Donnelly Centre, University of Toronto, 160 College Street, Toronto, Ontario M5S 3E1, Canada
[e] Lunenfeld-Tanenbaum Research Institute, Mount Sinai Hospital, Toronto, Ontario M5G 1X5, Canada
[f] Krembil Neuroscience Centre, Toronto Western Research Institute, and Department of Surgery, University of Toronto, 399 Bathurst Street, Toronto, Ontario, Canada M5T 2S8
[g] Department of Surgery, University of Toronto, Donnelly Centre, 160 College Street, Toronto, Ontario M5S 3E1, Canada

ARTICLE INFO

Article history:
Received 11 November 2015
Received in revised form
14 December 2015
Accepted 29 December 2015
Available online 1 January 2016

Keywords:
Cell adhesion molecules
Hydrogel
Differentiation
Induced pluripotent stem cells
Oligodendrocytes
Spinal cord injury
Cell transplantation

ABSTRACT

Transplantation of pluripotent stem cells and their differentiated progeny has the potential to preserve or regenerate functional pathways and improve function after central nervous system injury. However, their utility has been hampered by poor survival and the potential to form tumors. Peptide-modified biomaterials influence cell adhesion, survival and differentiation *in vitro*, but their effectiveness *in vivo* remains uncertain. We synthesized a peptide-modified, minimally invasive, injectable hydrogel comprised of hyaluronan and methylcellulose to enhance the survival and differentiation of human induced pluripotent stem cell-derived oligodendrocyte progenitor cells. Cells were transplanted subacutely after a moderate clip compression rat spinal cord injury. The hydrogel, modified with the RGD peptide and platelet-derived growth factor (PDGF-A), promoted early survival and integration of grafted cells. However, prolific teratoma formation was evident when cells were transplanted in media at longer survival times, indicating that either this cell line or the way in which it was cultured is unsuitable for human use. Interestingly, teratoma formation was attenuated when cells were transplanted in the hydrogel, where most cells differentiated to a glial phenotype. Thus, this hydrogel promoted cell survival and integration, and attenuated teratoma formation by promoting cell differentiation.

1. Introduction

Various cell types, including neural stem and progenitor cells (NPCs) derived from embryonic, fetal and adult human tissue, and more recently, from human induced pluripotent stem cells (hiPSC), have been transplanted in models of spinal cord injury (SCI) and have generated promising results [1–3]. Depending on the cell type, cell transplantation has been shown to promote neuroprotection via release of trophic factors, provide a growth-promoting matrix for regenerating axons, or replace lost cells. Notwithstanding, cell fate of donor cells has been typically poorly controlled, which has led to one of the major challenges in pluripotent cell transplantation – the potential to form teratomas.

Many conceptually different strategies to block teratoma formation have been pursued, including the introduction of suicide genes [4,5], selection of the desired cell type to increase purity [6], immunodepletion [7], cytotoxic antibodies [8] and selective ablation of pluripotent cells with small molecules [9]. While several of these strategies have been at least partially successful, guiding cell fate and cell purity prior to and/or after transplantation are key to success. For example, pre-differentiation into the oligodendroglial lineage has been shown to be more efficient for remyelination-mediated repair than grafting undifferentiated or uncommitted

* Corresponding author. The Donnelly Centre, 160 College St., Room 514, Toronto, Ontario M5S 3E1, Canada.
E-mail address: molly.shoichet@utoronto.ca (M.S. Shoichet).

http://dx.doi.org/10.1016/j.biomaterials.2015.12.032
0142-9612/

cells [10,11]. It has been demonstrated that human pluripotent stem cell-derived oligodendrocyte progenitor cells (OPCs) are capable of myelinating both axons in immunodeficient, dysmelinated shiverer mice [12], and spared axons in rats after spinal cord injury [13,14]. Moreover, OPC transplantation is the focus of a clinical trial in spinal cord injury [15].

One of the major challenges in cell transplantation to the central nervous system is cell survival. Dead or dying cells can worsen the outcome [16], necessitating delivery strategies that will improve the survival and integration of grafted cells [17]. Hydrogels have been shown to promote the survival of stem cells and their progeny [18,19]. Furthermore, hydrogels can be modified with peptide sequences and growth factors to further increase survival and/or promote differentiation. For example, the immobilization of both the cell-adhesive RGD peptide and the platelet-derived growth factor (PDGF-A) cytokine to a hydrogel increased the differentiation of rat NPCs into oligodendrocytes *in vitro* [20]. Interestingly, while the influence of extracellular matrix (ECM)-derived peptides on cell adhesion, differentiation and survival *in vitro* are well established, their effectiveness *in vivo* have been questioned [21–23].

We have previously demonstrated that a hyaluronan and methylcellulose (HAMC) hydrogel can be modified with growth factors and peptide sequences, and aid in cell transplantation of rodent cells after grafting into the retina, brain and spinal cord [19,20,24]. With a view towards enhancing survival of a clinically relevant cell source, in the present study we transplanted hiPSCs-derived OPCs in a rat model of spinal cord injury using HAMC modified with both the cell-adhesive RGD peptide and the cell survival and differentiation factor PDGF-A. We tested the effect of the RGD and PDGF-A modified hydrogel on cell survival and migration *in vitro* and *in vivo*, and its influences on cell fate *in vivo*.

2. Material & methods

2.1. Cell culture

Green fluorescent protein (GFP) positive hiPSCs were generated using the Piggy Bac transposon system, as described earlier [25] and differentiated into oligodendrocyte progenitor cells (OPCs) according to published protocols with slight modifications [12,26]. Briefly, hiPSCs were differentiated into neural stem cells under clonal (<10 cells/μl), serum free, minimal media conditions [27–29]. To induce differentiation into the oligodendrocyte lineage, neural stem cells were cultured as free-floating secondary neurospheres in neurobasal medium (Life Technologies) supplemented with 2% B27 without vitamin A (Life Technologies), 1 mg/ml transferrin, 0.09625 mg/ml putrescine, 0.25 mg/ml insulin, 0.06289 mg/ml selenium, 0.0518 mg/ml progesterone, 0.6% Glucose, 20 ng/ml of T3 (triiodothyronine), 100 ng/ml Biotin, 1 μM cAMP (cyclic adenosine monophosphate, all Sigma), 20 ng/ml PDGF-AA (platelet-derived growth factor), 20 ng/ml NT3 (neurotrophin-3, both Peprotech), and 1 μM Purmorphamine (EMD Millipore, OPC-media). Cells were cultured in a humidified incubator at 37 °C with 5% CO_2, fed every other day and larger spheres mechanically triturated once a week. Four weeks after differentiation of NPCs into OPCs, cells were tested for the expression of NKX2.2, OLIG2, PDGF-Receptorα and SOX10.

2.2. Flow cytometry and immunofluorescent staining

Eight well chamber slides (Thermo Scientific) were coated overnight at 37 °C with fibronectin (10 μg/ml, from bovine plasma, Sigma). The next day, fibronectin was removed and spheres (6–8/well) in 200 μl of OPC-media added. Cells were allowed to adhere overnight and fixed with ice cold 4% paraformaldehyde (PFA, Sigma) for 15 min. For flow cytometry spheres were incubated in Accutase (Sigma) for 10 min and mechanically dissociated into single cells [30], fixed in 4% PFA, subjected to immunocytochemistry and analysed using a BD Accuri C6 flow cytometer using excitation wavelengths of 488 and 640 with the following emission filter 533/30 nm (GFP) and 675/25 nm (Alexa647). Data was analysed using FlowJo (FlowJo, LLC) and the combined results of three independent experiments were plotted (n = 3, $1x10^4$ cells per antibody/experiment). To estimate the percentage of positively expressing cells, a gate was set based on the negative control so that only 1% are considered within this gate [31]. Cells and spinal cord sections were stained according to standard protocols [32,33]. For a complete overview of all antibodies/counterstains used, see supplemental Table 1. Primary antibodies were diluted in PBS-T (Phosphate Buffered Saline with 0.05% Tween 20) and incubated with the samples overnight at room temperature. Primary antibodies were detected by incubation with fluorescence secondary antibodies for 2.5 h at room temperature. Cell nuclei were counterstained with 4,6-diamidino-2-phenylindole dihydrochloride (DAPI; 1 μg/ml, Invitrogen). Samples were covered with a coverslip using ProlongGold (Life Technologies) and visualized using a confocal microscope (Olympus FV1000) at 20x (NA 0.75) magnification to create overviews or at 40x (NA 0.6) magnification for demonstration of cell fate.

2.3. PCR

RNA was extracted from OPCs and NPCs using Trizol (n = 3 for NPC, n = 5 for OPC), according to the manufacturer's protocol (Life Technologies) and stored at −80 °C. Samples were treated with enzyme Turbo DNase for 30 min in a water bath at 37 °C to eliminate genomic DNA contamination of the RNA samples, resuspended in deactivation buffer, shaken for 5 min and centrifuged at 4 °C at 10,000 g for 1.5 min. The supernatant was collected and total RNA estimated using Nanodrop. Pure RNA was reverse transcribed into cDNA using SuperScript Vilo cDNA Synthesis Kit according to the manufacturer's protocol. Subsequently, the PCR product was diluted with RNase-free water and 2 μL (2.5 ng/μL) were used for each reaction. Primers used were: OLIG2, PDGF-Receptorα, NKX2.2, SOX10, and GAPDH (housekeeping gene, see supplemental Table 2 for primer sequences). For quantitative real time PCR (qPCR) the Roche lightcycler 480 SYBR Green I Master mix was used following the manufacturer's instructions using an ABI 7900 HT machine (Applied Biosystems).

2.4. Hydrogel

Methyl cellulose (MC, M_w 310 kDa, Shin-Etsu Metolose SM-4000, Japan) conjugated with peptide and PDGF-A was prepared as previously described [20]. Briefly, MC was first chemically-modified to introduce a reactive thiol that was then sequentially reacted with maleimide–streptavidin and maleimide–peptide by Michael-type addition. Biotin-modified recombinant PDGF-A, expressed in E. coli and biotinylated according to established methods [20], was then immobilized to the streptavidin portion of the modified MC polymer. Maleimide-peptides were synthesized using an automated peptide synthesizer. Since it has been demonstrated that longer peptide sequences have greater biological activity/binding capacity than shorter sequences [34], we used the peptide sequence Ac-GRGDS-PASSK-G_4-SR-L_6-R_2KK(Maleimide)G, where RGD is the fibronectin-derived adhesion sequence. To enable the conjugation of multiple peptide/protein components to the same polysaccharide chain, limiting amounts of streptavidin relative to reactive thiols present in methyl cellulose (~1 mol maleimide (bound to streptavidin)/100 mol free thiols

bound to MC) were used. Unreacted free thiols were then reacted with a second desired maleimide-containing component in a subsequent step (i.e. Maleimide-RGD peptide). Hyaluronan (HA, MW 1500 kDa, Dramen, Norway) and MC or MC-PDGF-A/-RGD were dissolved in double distilled, deionized water, sterile filtered, lyophilized and stored at −20 °C under sterile conditions. HA and MC, MC-RGD/PDGF-A or MC-RGD were weighed on an analytical balance in a biosafety cabinet under sterile conditions. Media was added to HA and MC, MC-RGD/PDGF-A or MC-RGD (1% w/v), and gently agitated overnight at 4 °C. The dissolved hydrogel was mixed in a speedmixer for 20 s at 3500 RPM, followed by centrifugation at 14,400 RPM for 45 s and cooled on ice until cell addition. HAMC was mixed with the cell solution at a ratio of 1:1 to achieve a final concentration of 0.5%/0.5% (HA/MC, w/v), resulting in a physical blend of HA and MC in media. As MC forms a loosely crosslinked network through hydrophobic interactions, no crosslinker was added.

2.5. In vitro investigations

The OPCs were cultured as spheres within peptide-modified HAMC (0.5%/0.5% w/v) gels at a MC to MC-peptide ratio of 3:1 (6–8 spheres/well using 8 well chamber slides). OPCs were cultured for 7 days without media changes and tested for cell adhesion/migration and viability. Cell viability was characterized by calculating the percentage of live cells using the GFP signal for viable cells and ethidium homodimer for dead cells (1:250, Life Technologies). Z-stacks were taken using a live cell incubation chamber (10x objective, 37 °C, 5% CO_2) attached to an inverted Olympus confocal laser scanning microscope and ImageJ. Migration was quantified by counting the numbers of cells that detached from the seeded sphere and changed their morphology from the rounded, process-less, phenotype to a flattened cell morphology with extending processes. Cell-substrate interactions were determined by the number of cells migrating away from the spheres. OPCs cultured in HAMC-RGD were compared to unmodified HAMC and normal tissue culture plastic (uncoated; n = 3, 4 gels for each replicate). Cells in all conditions were cultured in OPC-media including PDGF-A to determine the effect of MC-RGD on cell survival and migration. PDGF-A was necessary to ensure at least minimal cell survival in all groups. Previous results demonstrated that conjugated and soluble PDGF-A had similar effects on cell survival and differentiation [20,24,35], therefore only soluble PDGF-A was used in these *in vitro* studies.

2.6. Spinal cord injury

All animal procedures were performed in accordance with the Guide to the Care and Use of Experimental Animals (Canadian Council on Animal Care) and protocols were approved by the Animal Care Committee of the Research Institute of the University Health Network. 54 Female Sprague Dawley rats (300 g, Charles River, Montreal, QC) were used to assess the effects of cell transplantation in terms of cell survival, integration and fate, and animal behavioural function. Three groups were compared: (I) artificial cerebrospinal fluid (aCSF); (II) OPCs in media; and (III) OPCs in HAMC-RGD/PDGF-A. Clip compression injury was performed as described previously [36]. Briefly, animals were anaesthetized and subjected to a laminectomy at level T2. The spinal cord was injured by cord compression with a 24 g modified aneurysm clip for 1 min, resulting in a moderate SCI [37]. After closing the overlying muscles, fascia and skin, rats were placed under a heating lamp and allowed to recover.

2.7. Artificial cerebrospinal fluid

To mimick the physiological ion concentrations of the CSF we used artificial CSF comprised of: 148 mM NaCl, 3 mM KCl, 0.8 mM MgCl2, 1.4 mM $CaCl_2$, 1.5 mM Na_2HPO4, 0.2 mM NaH_2PO_4, and 0.1 mg/ml bovine serum albumin [38].

2.8. Cell transplantation and sacrifice

All rats underwent a second operative procedure 7 days after injury. Rats were anaesthetised as described above, and the previous operative site re-exposed. Injections were made stereotactically through the intact dura with the aid of an operating microscope using a motorized microinjector at a rate of 1 μl/min. A total of 4 injections were made using a 10 μl Hamilton syringe with a customized 32 gauge needle: 2 injections, 1 mm rostral and 2 injections, 1 mm caudal from the lesion site, each 1 mm lateral from the midline, containing 2 μl of aCSF (control) or cells in media or HAMC-RGD/PDGF-A (1×10^5 cells/μl). Hydrogels were prepared as described above. The needle was left in place for an additional 2 min after injection to prevent cell leakage. To aid transplant survival, all animals (including the non-cell controls) were given cyclosporine A (Sandimmune, Novartis Pharma, Canada Inc, Dorval, Quebec, Canada) via subcutaneous implanted osmotic pumps (Alzet) starting one day prior to transplantation until sacrifice. For the two week survival time point, pump model 2ML1 was used, which delivered cyclosporine A at a rate of 10 μl/h for 1 week. For the 8 week survival time point, pump model 2ML4 was used, which delivered cyclosporine A at a rate of 2.5 μl/h for 4 weeks. Both pumps delivered cyclosporine A at a final concentration of 10 mg/kg/day. To aid in cell survival for the entire duration of the long term study pumps were replaced with new pumps after 4 weeks. Animals were sacrificed and transcardially perfused with 4% PFA in 0.1 M phosphate buffer (PB, pH 7.4) at 2 weeks and 9 weeks post injury (wpi), the spinal cords removed, cut into blocks of 1.5 cm encompassing the site of injury/injection and processed for serial longitudinal cryosectioning (20 μm) to investigate cell survival, cell fate and tissue repair (n = 6 per group at 2 wpi, n = 3, 4, 6 for OPC-media, OPC-HAMC-RGD/PDGF-A, and the control group, respectively at 9 wpi).

2.9. Housing and post-operative care

Buprenorphine (0.05 mg/kg) was administered twice daily every 12 h for 48 h after surgery. One animal was housed per cage in a temperature-controlled room with a 12 h light/dark cycle for 2 or 9 weeks after injury. Clavamox was added to the water for 1 d pre-operatively and for 5 d post-operatively to prevent urinary tract infections. The bladders were manually expressed 3 times per day until bladder function returned. Water and food were provided ad libitum. Skin clips were removed 10–14 d post-operatively.

2.10. Morphological investigations

Image overviews encompassing the lesion site/transplanted cells were taken using a motorised stage and the same settings for all groups. At 9 wpi some grafted cells had spread out so far that complete overviews could no longer be taken, instead smaller overviews from different regions of the sections were taken. Longitudinal sections evenly distributed throughout the entire thickness of each rat spinal cord were used for analysis by a user blinded to the treatment. Due to the high density, the number of transplanted cells found at 2 wpi was estimated by dividing the total number of the GFP+ area by the average size of a transplanted cell (calculated from >1000 cells). Cell survival as a percentage was

estimated by dividing the amount of cells observed by the number of cells injected and the result multiplied by 100% ($n \geq 19$ sections/animal). Ki67 was used to identify proliferating cells. For comparison between the two cell transplant groups, the total number of Ki67 and GFP double positive cells in three overviews per animal was counted. The average number of Ki67/GFP double positive cells was plotted. The extent of migration at 2 wpi was estimated by measuring the length of the perimeter of the area enclosing the GFP+ cells for the individual injections (continuous cell cluster) ($n \geq 19$ sections/animal) [39]. Multiple overlays of the GFP+ cells were converted to black and white and combined to create an image depicting the overall spread of cells. Lesion size at 9 wpi for the control group was estimated according to the GFAP staining and plotted as cystic cavitation. Cells transplanted in media created multiple cystic-like epithelial structures. The area covered by these cysts was added up and counted towards the cystic cavitation ($n \geq 3$ sections/animal). To quantify how many animals had teratomas, sections were stained for mesodermal (α-smooth muscle actin (SMA)-positive) and endodermal (alpha-fetoprotein (AFP)-positive) marker. Furthermore, to estimate the amount of cells differentiating into non-neural tissue, we identified four morphologically distinct structures usually not found in the spinal cord, even after injury: (1) elongated cells, possibly muscle cells, (2) very dense clusters of small cells, possibly cartilage, (3) thick square cells, forming a tubular structure within the cord, possibly liver or gut, and (4) thinner square cells, forming larger hollow structures, possibly endothelial cells and counted them using a standard fluorescence microscope (200x magnification, Olympus, $n \geq 8$ sections/animal) [5,9,40].

2.11. Behavioural test

For animals surviving 9 weeks, motor behaviour was evaluated weekly by two blinded observers using the Basso, Beattie and Bresnahan (BBB) locomotor rating scale [41] ($n = 8$, 8, and 10 for OPC-media, OPC-HAMC-RGD/PDGF-A, and the control group, respectively).

2.12. Statistical analysis

Data are plotted as mean ± standard error of the mean (SEM). For comparison between the two cell groups at 2 wpi, data were compared by a t-test. For multiple comparisons between pairs of means for *in vitro* investigations, behavioural analyses and size of cystic cavitations at 9 wpi, data were compared by an analysis of variance (ANOVA) followed by a Bonferroni's test. p values of <0.05 were regarded as significant ($^{*}p < 0.05$, $^{**}p < 0.01$, $^{***}p < 0.001$). All tests were performed using the statistical software GraphPad Prism version 5.0.

3. Results

3.1. Cell characterisation

Human iPS-derived NPCs were differentiated for 4 weeks as spheres, which appeared as large, tightly bound clusters of cells. When plated onto fibronectin-coated substrates, spheres rapidly adhered and flattened, and cells with a bipolar morphology migrated away in a radial pattern. The combined expression of Olig2, NKX2.2, PDGF-Rα and SOX10 identified the cells as OPCs. While iPS-cells demonstrated a nuclear expression of Nanog, OPCs were Nanog-negative (supplemental Fig. S1A, B). Immunocytochemistry of the OPCs demonstrated that only PDGF-Rα was distributed at the cell membrane, whereas SOX10, NKX2.2 and Olig2 were nuclear, with Olig2 visible in fine processes as well (Fig. 1A–D, red). Interestingly, NKX2.2 demonstrated variable staining intensity (Fig. 1C). The bipolar morphology was most clearly visible in cells farther away from the centre of the sphere (e.g. cells at the top of Fig. 1D). Quantification using flow cytometry showed the average number of cells expressing SOX10 (90%), PDGF-Ra (77.4%), NKX2.2 (84.1%) and Olig2 (98.3%, Fig. 1E–H). qPCR showed the corresponding mRNA upregulation (compared to NPCs), demonstrating that the cells expressed all four markers and that the corresponding genes were significantly upregulated (Fig. 1J–M).

3.2. Influence of RGD on cell survival in vitro

To investigate the role of the RGD peptide on cell survival, OPCs were cultured *in vitro* within HAMC-RGD, HAMC and on non-coated tissue culture plastic (TCP) controls for 1 week in media supplemented with PDGF-AA. OPCs grown in HAMC-RGD migrated away from the seeded spheres, which were embedded within the hydrogel, indicating excellent cell–substrate interactions. In stark contrast OPCs grown in unmodified HAMC remained predominantly as spheres, with low survival of single cells, indicating greater cell–cell vs. cell–substrate interaction (Fig. 2A, B). OPCs on TCP showed poor survival, with the remaining surviving cells adhering to the bottom of the plate and migrating away from the spheres (Fig. 2C). RGD peptide modification of the hydrogel led to significantly greater cell survival compared to HAMC and TCP ($p < 0.001$), but there was no difference between cells cultured in HAMC vs. TCP (Fig. 2D). Furthermore, cells grown within HAMC-RGD and on TCP had significantly more migrating cells than cells grown in HAMC (Fig. 2E).

3.3. Cell survival and migration in vivo at 2 weeks post injury

Next, we compared the ability of the RGD and PDGF-A modified HAMC to promote cell survival and integration *in vivo* compared to cells transplanted in media at 2 wpi (7 days after grafting). Fluorescence microscopy showed many viable cells in both groups, most of which expressed the OPC marker SOX10 (Fig. 3A, B). However, some of the cells also expressed the proliferation marker Ki67 (Fig. 3C, D), but not Oct4 (supplemental Fig. S1C, D). Significantly more cells were found when transplanted in HAMC-RGD/PDGF-A (Fig. 3E), with approximately 46% of the initial cell number compared to 29% of the initial cells transplanted in media (Fig. 3F). Interestingly, significantly more proliferating cells were found in cells transplanted in media than in the hydrogel (Fig. 3G), indicating that the number of viable cells in the media could be attributed to proliferation whereas the higher number of viable cells in the hydrogel could be attributed to survival.

The majority of cells in both groups migrated away from the injection site (asterisk) towards the injury site, where they formed large clusters (Fig. 4A, B). As expected, migration was seen predominantly in the white matter (Fig. 4C). This was especially visible when the injection occurred partly in the grey matter (GM) and the cells only migrated in the white matter (arrow, Fig. 4C). The migrating cells indicate cell–substrate interactions, although evidence for migration was lacking in 1/3 of the injections sites in the OPC-media group (Fig. 4A, circle). Interestingly, migration away from the injection site was significantly greater in the OPC-HAMC-RGD/PDGF-A group (Fig. 4D, $p < 0.001$). There was extended migration rostral and caudal to the injury/injection site (Fig. 4E), where cells were found in close proximity to ED1+ immune cells (Fig. 4F). The enhanced migration was reflected in better integration as determined by the intermingling of the grafted cells with host astrocytes and axons; however, this difference was not significant ($p > 0.05$, supplemental Fig. S2A-F).

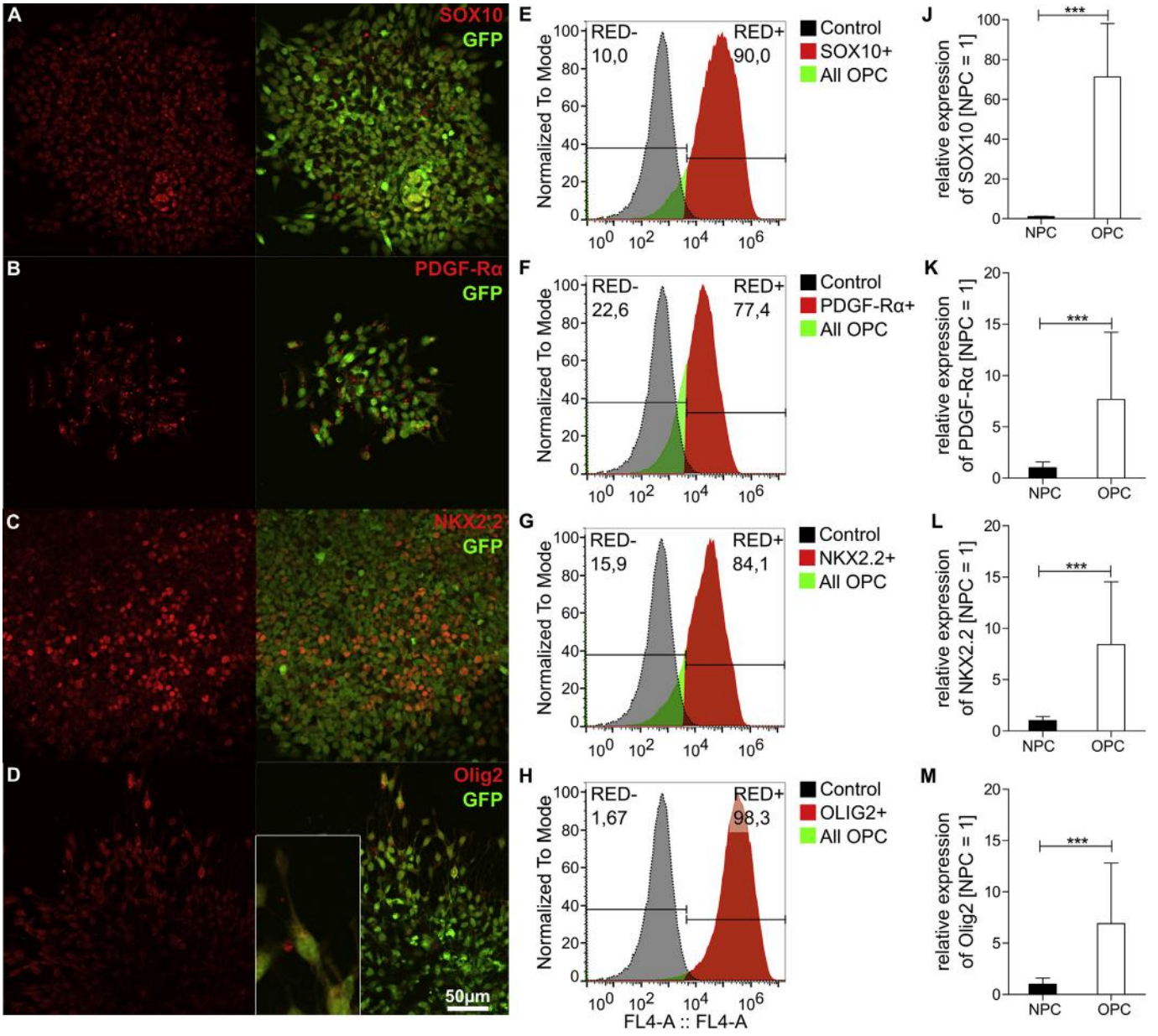

Fig. 1. Flow cytometry and qPCR demonstrate the successful differentiation of NPCs into OPCs. Immunofluorescence images of representative examples of differentiated cells (GFP, green), stained (A) SOX10 (red), (B) PDGF-Receptorα (red), (C) NKX2.2 (red), and (D) Olig2 (red). Insert in (D) demonstrate the bipolar morphology. (E–F) Quantification with flow cytometry demonstrates the amount of positive cells (%) for the respective marker (n = 3, 1 × 10^4 cells per antibody/experiment). qPCR demonstrates the upregulation of (J) SOX10, (K) PDGF-Receptorα, (L) NKX2.2, and (M) Olig2 compared to undifferentiated NPCs (n = 3 for NPC, n = 5 for OPC). Data represents mean ± SEM, ***$p < 0.001$. Scale bar in (D) for (A–D). (For interpretation of the references to colour in this figure legend, the reader is referred to the web version of this article.)

3.4. Cell distribution, fate and cystic cavitation at 9 weeks post injury

Animals receiving aCSF demonstrated large cavitations at 9 wpi with clearly delineated GFAP-positive astrocytes lining the glial scar (Fig. 5A). Cell-free hydrogel controls showed similar cystic cavitation and scar formation as aCSF controls (supplemental Fig. S3A-C). Cells transplanted in media filled the lesion site and surrounding tissue completely, but demonstrated heterogeneous cell morphology (Fig. 5B). Furthermore, multiple small cavitations were observed in the tissue. Cells transplanted with HAMC-RGD/PDGF-A showed a more homogeneous cell morphology in most animals and filled the lesion site completely (Fig. 5C). On average this group had significantly smaller cystic cavitation compared to the non-cell control group (Fig. 5D, $p < 0.01$). Higher magnification revealed that cells at the host-graft border differentiated into GFAP+ astrocytes and that there was limited (if any) glial scarring in the OPC-HAMC-RGD/PGDF-A group (Fig. 5E, dashed line). Although cells in the OPC-media group also differentiated into and/or intermingled with host astrocytes, there was a recognisable segregation (Fig. 5F), albeit not as clear cut as the glial scar in the non-cell groups (Fig 5A). The majority of cells grafted within the hydrogel still expressed markers associated with astrocytes (GFAP, Fig. 5E) or OPCs (e.g. SOX10, Fig. 6A), with only few cells expressing MBP, SOX2, SMA or AFP (Fig. 6A, B, C). Cells transplanted in media were more heterogeneous, with only rare occurrence of OPCs (Fig. 6D). The majority de-differentiated into large, polygonal CD44-positive, vimentin-positive, and GFAP-negative cells, possibly

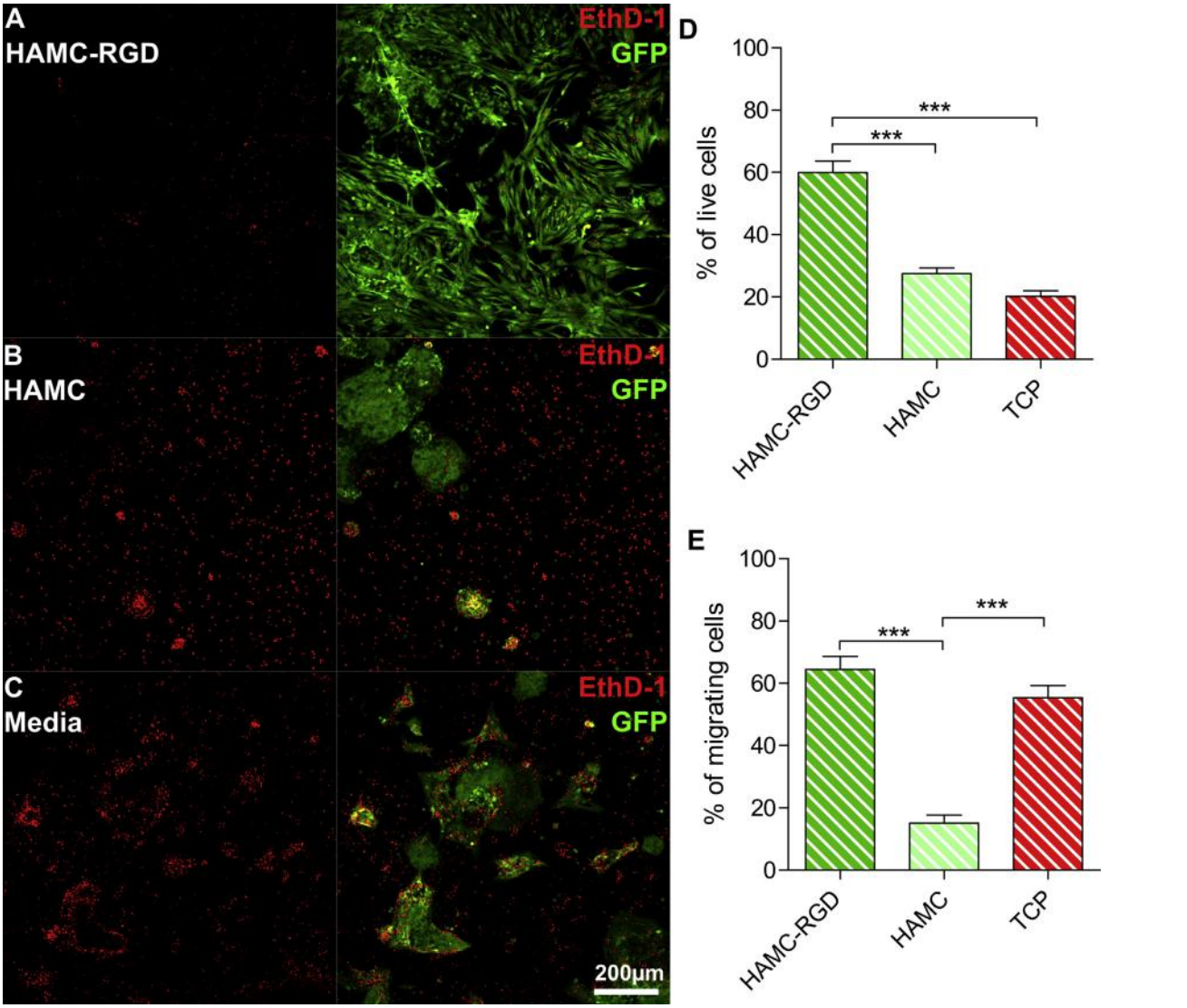

Fig. 2. RGD promotes the survival of OPCs in vitro. Representative images of OPCs (green) cultured in (A) HAMC-RGD, (B) unmodified HAMC, and (C) tissue culture plastic (TCP). (D) Analysis of the cell viability with GFP (green) for live cells and ethidium homodimer (EthD-1, red) for dead cells demonstrated increased cell survival within HAMC-RGD compared to HAMC and TCP. (E) Furthermore, the RGD peptide promoted greater migration than HAMC, but not significantly more than TCP. Media was supplemented with PDGF-AA in all groups. Data represents mean ± SEM, n = 3, 4 gels for each replicate ***$p < 0.001$. (For interpretation of the references to colour in this figure legend, the reader is referred to the web version of this article.)

fibroblasts (Fig. 6E, supplemental Fig. S4A, B), and also differentiated into cells of other germ layers, as indicated by AFP- and SMA-positive immunostaining (Fig. 6F). All animals receiving cells in media (100%) vs 50% of those receiving cells in HAMC-RGD/PDGF-A demonstrated signs of teratoma formation. Cells transplanted in media demonstrated a high occurrence of non-spinal cord structures, which were all derived from the grafted cells (GFP-positive, Fig. 7A). While structures with epithelial cellular characteristics in the OPC-HAMC-RGD/PDGF-A group were found, their occurrence was significantly lower than that in animals receiving cells in media (Fig. 7B, C), neither muscle nor cartilage tissue was observed.

3.5. Behavioural outcome at 9 weeks post injury

Animals demonstrated normal locomotor behaviour prior to the injury (BBB score of 21), with a significant drop after clip compression spinal cord injury, where animals were only able to partly move their hindlimbs (average BBB score of 4, prior to cell injections). Animals recovered to an average BBB score of 10.8 for the OPC-HAMC-RGD/PDGF-A group, 10.2 for the aCSF control group, and 7.9 for the OPC-media group. Interestingly, animals that received cells in media demonstrated a decline in motor function at 6 wpi and were significantly worse than animals in the OPC-HAMC-RGD/PDGF-A group at 8 and 9 wpi (Fig. 7D, $p < 0.05$), but only worse than the aCSF group at week 8 ($p < 0.05$). Animals injected with cell-free hydrogel controls demonstrated a similar behavioural outcome to those injected with aCSF (average BBB: 9.9, supplemental Fig. S5A).

4. Discussion

We demonstrate that HAMC-RGD/PDGF-A promotes the early survival of human iPS-derived OPCs after transplantation into the injured spinal cord and attenuates teratoma formation of hiPS cells by promoting their differentiation compared to cells transplanted in media. We attribute the beneficial effects of the hydrogel to the

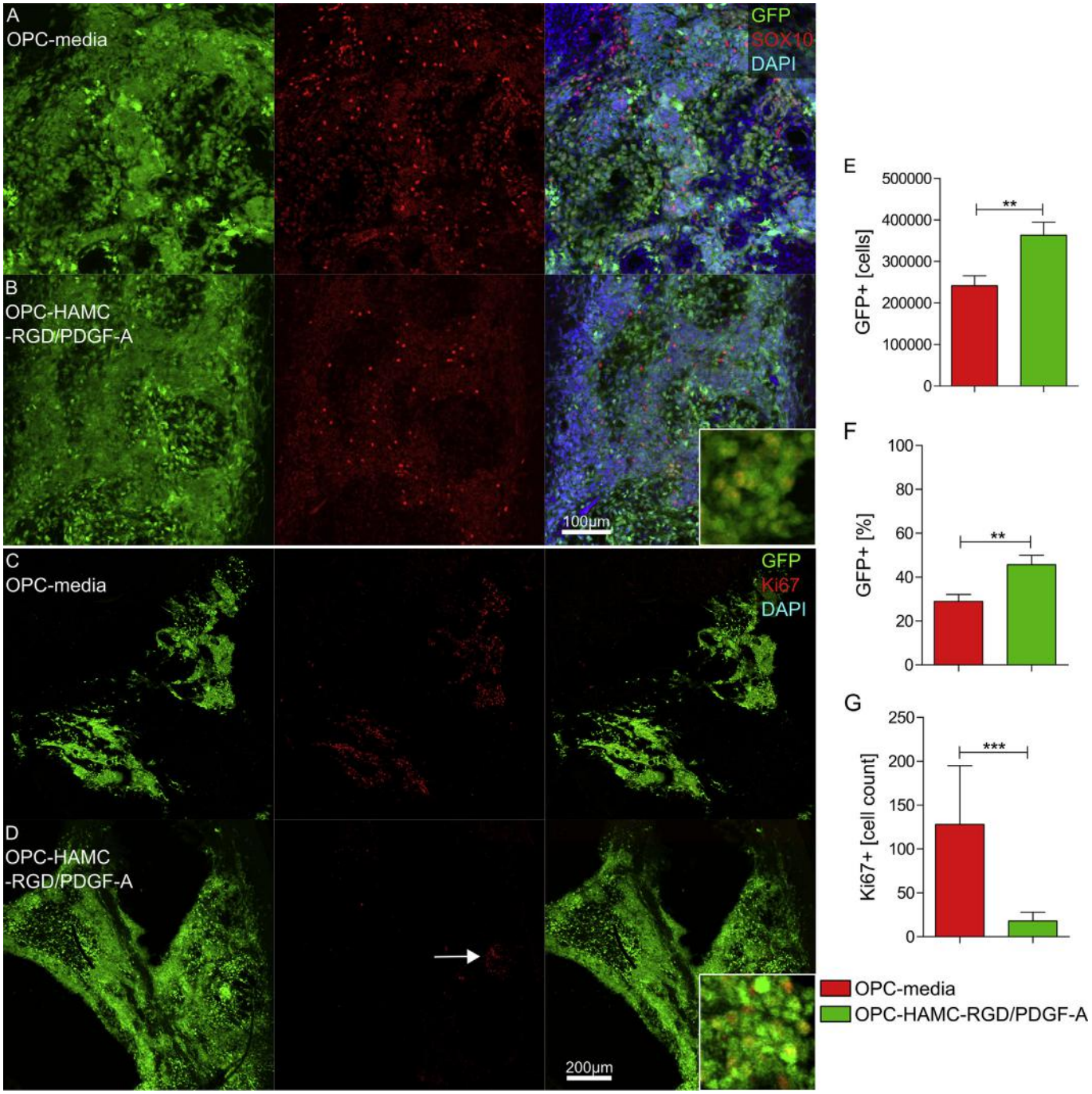

Fig. 3. HAMC-RGD/PDGF-A promotes early cell survival in rat spinal cord injury model. Cells transplanted in (A) media and (B) HAMC-RGD/PDGF-A expressed the OPC marker SOX10; and the proliferation marker Ki67 (C, D) at 2 wpi. Significantly more cells were found when they were grafted in the hydrogel as shown for both (E) numbers and (F) % of injected GFP+ cells, although (G) more proliferating cells were found when grafted in media. Inserts represent higher magnification images of the staining presented. Images shown were taken at the lesion site. Data are plotted as mean ± SEM, n = 6 animals/group $^{**}p < 0.01$, $^{***}p < 0.001$. Scale bar in (D) for (A–D).

peptide and growth factor modification of HAMC, based on our previous observations where only cell survival and not cell differentiation were observed with rodent cells in HAMC [20,24,42] and the *in vitro* results presented herein of enhanced migration and survival in RGD-modified HAMC.

While a number of protocols for the differentiation of human induced pluripotent stem cells to oligodendrocyte progenitor cells have been published [12,26,43], the process is lengthy, usually taking more than 3 months. This might hinder their clinical utility as a treatment for spinal cord injury, especially if the goal is to use autologous cell transplants, since the time window for beneficial cell transplantation might be shorter than the differentiation protocols [14]. Here, cells were characterised after four weeks in differentiation media, when they started to express NKX2.2, Olig2, SOX10 and PDGF-Rα, which identified them as OPCs similar to previous reports [12,26,43]. Longer differentiation times are needed for greater lineage commitment or to generate mature oligodendrocytes, which lose the ability to migrate and remyelinate spared axons [14,44]. Our immature OPCs maintained the ability to myelinate spared axons, as we observed, but this was at the cost of

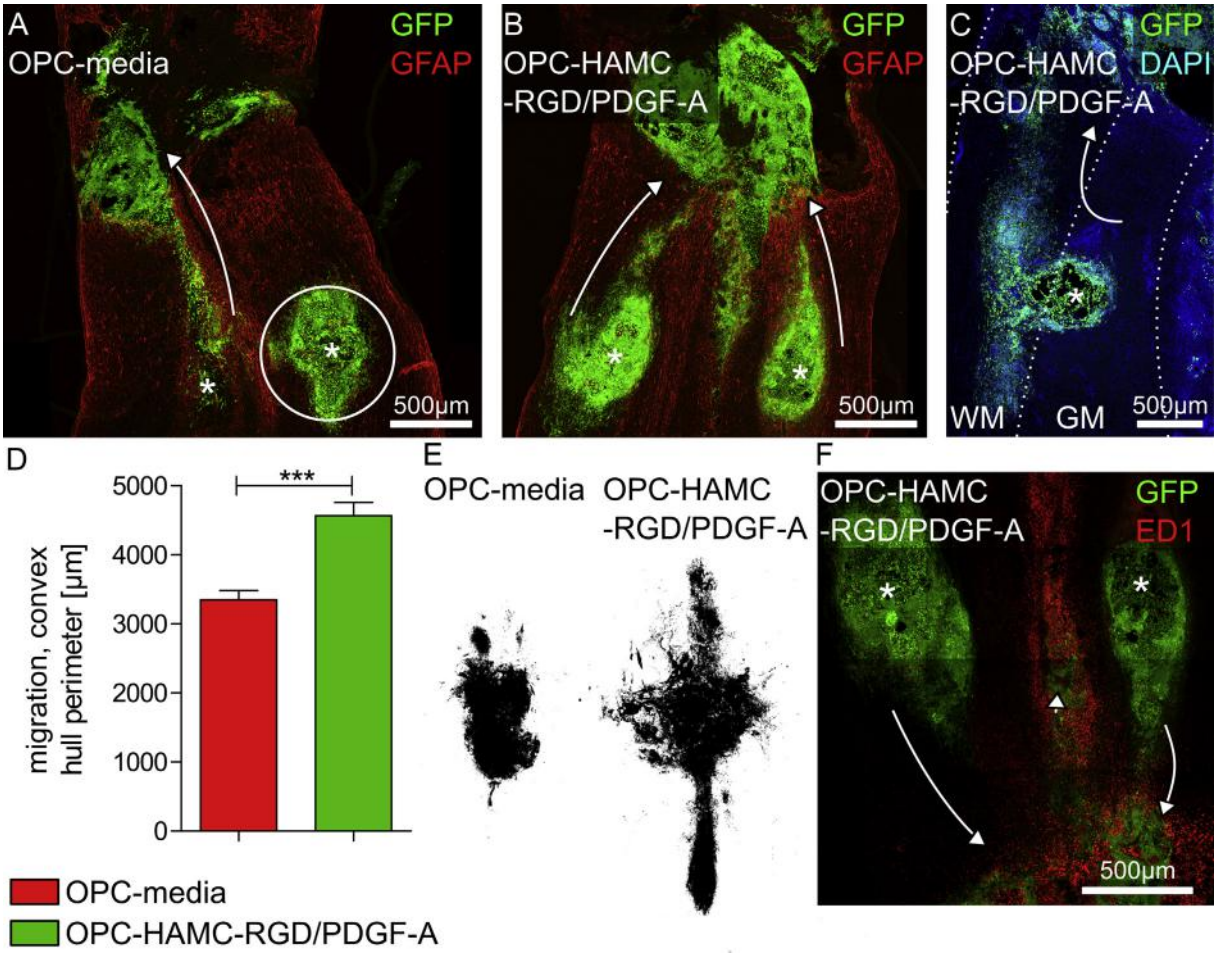

Fig. 4. HAMC-RGD/PDGF-A promotes cell migration at 2 wpi. Injected cells in (A) media and (B) HAMC-RGD/PDGF-A migrated away from the injection (asterisk) towards the lesion site (arrows). No migration was observed in 1/3 of the injections for cells grafted in media (A, circle). (C) As expected, most migration occurred in the white matter (WM). This was especially visible when the injection occurred partly in the grey matter (GM) and the cells only migrated in the white matter (arrow). (D) Interestingly, cells migrated further when transplanted in HAMC-RGD/PDGF-A, which appears to be due, in part, to (E) migration along the midline rostral and caudal to the injury site, in close proximity to (F) ED1+ cells. (E) Multiple overlays of the GFP+ cells were converted to black and white and combined to create an image depicting the overall spread of cells. Data are plotted as mean ± SEM, n = 6 animals/group ***$p < 0.001$.

teratoma formation in 100% of animals with OPCs delivered in media, yet only 50% of animals with OPCs delivered in HAMC-RGD/PDGF-A.

A critical challenge for the success of any cell-based therapy is the enormous degree of cell death following transplantation [45,46] and human stem cell transplantation into the injured spinal cord of immunocompetent animals has resulted in only limited cell survival [17]. Cyclosporine A was used to minimize the rejection response by the host immune system and to allow successful engraftment and survival of the transplanted cells. A rejection response itself may alter the efficacy and safety profile of the grafted cells. In the absence of good engraftment conditions, a valid analysis of the tumorigenic potential of pluripotent-derived cells may not be possible [17,47].

Biomaterials can positively influence cell survival and earlier studies demonstrated anti-inflammatory and pro-survival effects of HA [48–50]. Furthermore, HAMC was able to improve the survival of rodent NPCs both *in vitro* during their storage on ice prior to transplantation and *in vivo* after acute injections [19]. In particular interactions through CD44, a receptor for HA, have been shown to be critical to cell survival, growth, migration, and differentiation [19,51,52]. However, CD44 is thought to identify astrocyte restricted precursor cells within neural progenitor cell populations and is not expressed on OPCs [53,54]. Furthermore, rodent NPCs within HAMC-PDGF-A did not demonstrate increased survival compared to unmodified HAMC *in vitro* or compared to media *in vivo* in an experimental animal model of SCI [24]. Therefore, neither HAMC-PDGF-A nor HAMC alone seems to be sufficient to promote OPC survival. In contrast, we observed significant survival of OPCs at 2 wpi in HAMC-RGD/PDGF-A vs. media and attribute this to RGD. RGD promotes cell adhesion which is critical to cell survival, proliferation, differentiation and migration [55]. The lack of an adhesive substrate leads to anoikis – programmed cell death due to a lack of extracellular matrix [56,57]. Short, cell adhesive peptides, like RGD, mimic the extracellular microenvironment and increase cell adhesion and survival [58,59]. This biomimicry is enhanced with longer amino acid sequences, such as the RGD-sequence that we used: Ac-GRGDS-PASSK-G4-SR-L6-R2KK(maleimide)G. The RGD-modified hydrogel promoted not only greater survival of OPCs, but also their migration (compared to cells grafted in media), which mirrors our observations *in vivo*, demonstrating the beneficial effect of the peptide sequence *in vitro* and *in vivo*.

We observed enhanced migration from the injection site to the lesion site of the OPCs delivered in HAMC-RGD/PDGF-A compared to cells in media at 2 wpi. This is consistent with the positive effect of fibronectin on cell migration that has been demonstrated

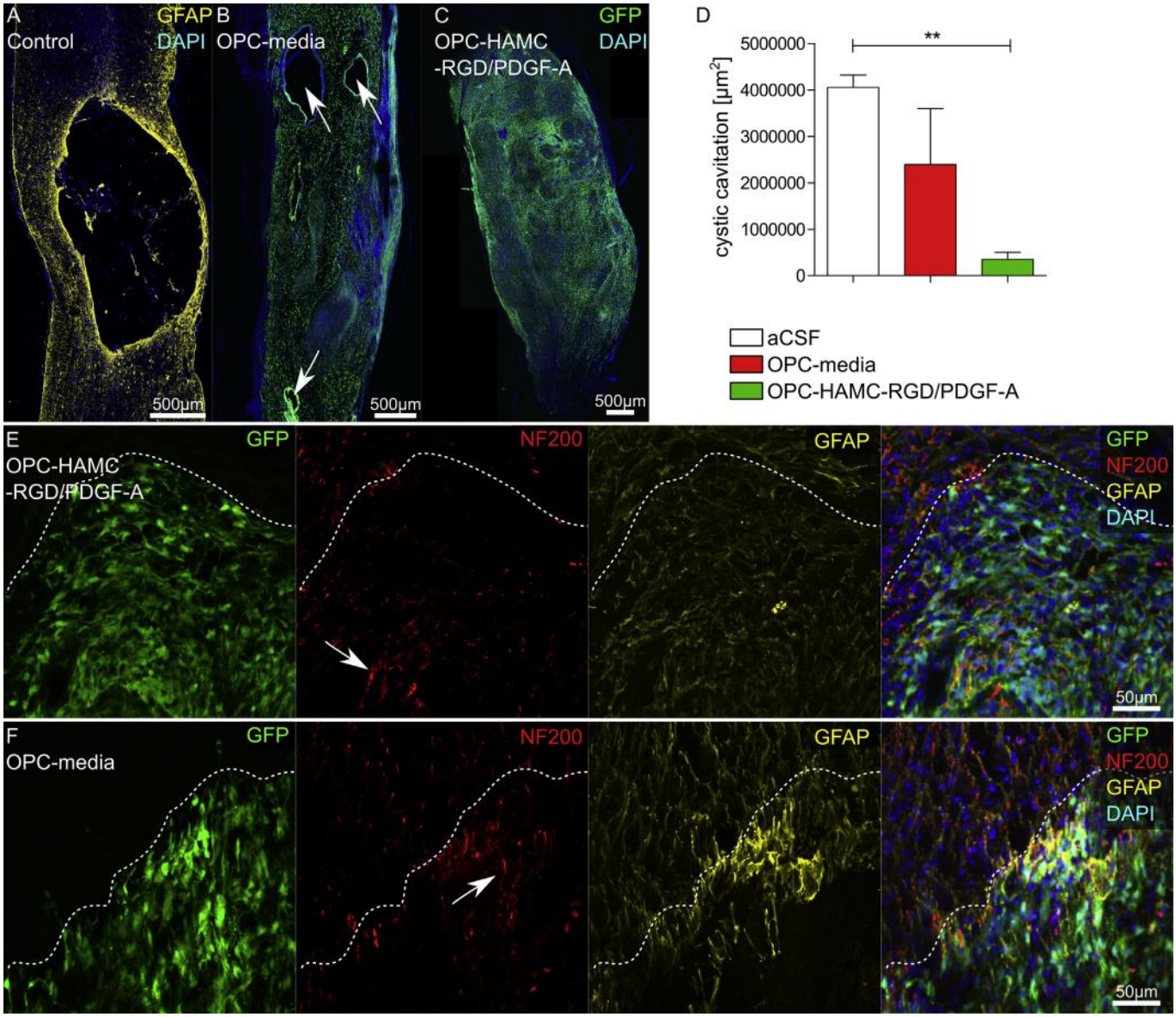

Fig. 5. Cells in HAMC-RGD/PDGF-A reduce cystic cavitation at 9 wpi. (A) Cavity and scar formation in animals receiving aCSF (control). OPCs (green) transplanted in (B) media and (C) HAMC-RGD/PDGF-A were found throughout the tissue. (B) Cells in media formed cystic-like epithelial structures (arrows), which were counted towards cystic cavitation. (D) Only cells transplanted in HAMC-RGD/PDGF-A significantly reduced cystic cavitation. Data are plotted as mean ± SEM, $n \geq 3$ sections/animal, $^{*}p < 0.05$, $^{**}p < 0.01$. (E) Higher magnification at the graft-host border (*dashed line*) revealed that OPCs differentiated into GFAP-positive astrocytes (yellow) in the OPC-HAMC-RGD/PDGF-A group. (F) There was a more visible segregation between transplanted cells and host tissue. (E, F) Axons (red, NF200) were able to extend processes into the graft (arrows). (For interpretation of the references to colour in this figure legend, the reader is referred to the web version of this article.)

previously [60,61]. Interestingly, migrating OPCs were associated with ED1-positive cells. While it has been demonstrated previously that inflammatory cells can promote the migration of OPCs [62,63], it is unclear which cell type attracted the OPCs, as factors secreted by host cells, which attracted the immune cells, might have attracted the OPCs as well. Regardless of the initial attraction, this might have implication for remyelination-based repair after spinal cord injury. Migration of OPCs to spared axons of demyelinating lesions enables them to remyelinate the axons; however, here the majority migrated into the lesion site, which lacks axons. While it has been demonstrated that NG2-positive OPCs can support axonal outgrowth [64], other substrates might promote greater axonal regeneration. Nonetheless, the cells would be able to remyelinate regenerating axons crossing the lesion site.

The enhanced migration of cells delivered in HAMC-RGD/PDGF-A vs. media was reflected in better integration as determined by the intermingling of the grafted cells with host astrocytes and axons; however, this difference was not significant ($p > 0.05$). Grafted cells had not differentiated into astrocytes or neurons at this time point (2 wpi). Typically, OPCs would integrate through the mechanism of remyelination of spared axons; however, we also observed axonal growth along OPCs into the lesion site, similar to what others observed with NG2-positive oligodendrocyte progenitor cells, which provided a substrate for regenerating axons [64]. MBP expression was increased in the HAMC-RGD/PDGF-A group, but this was mostly associated with host cells rather than grafted cells and similar to previous observations [24]. This suggests that the immobilized PDGF-A can also interact with host cells to promote their survival and maturation, as has been suggested previously [24]. No differences between the groups were observed in terms of

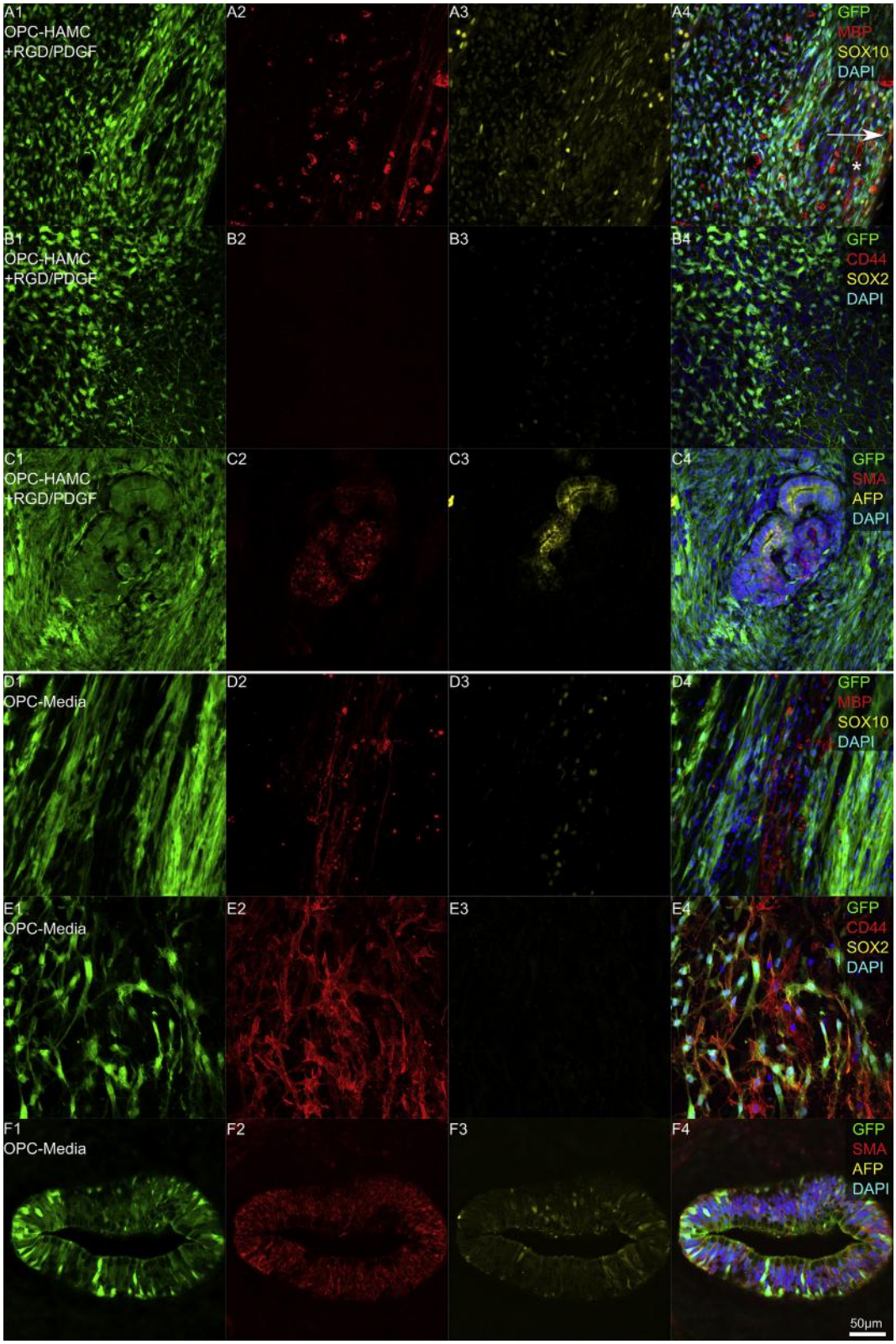

Fig. 6. HAMC-RGD/PDGF-A promotes glial differentiation. (A) Cells transplanted in HAMC-RGD/PDGF-A mostly co-localized with markers of the glial lineage (MBP, red; SOX10, yellow), but not with (B) CD44 (red) or SOX2 (yellow). Asterisk in (A) indicates endogenous MBP whereas arrow indicates area of grafted cell myelination. (C) Few, if any SMA (red, mesodermal marker) or AFP (yellow, endodermal marker) positive cells could be found. (D) Most cells transplanted in media did not express MBP or SOX10, but (E) rather CD44, possibly de-differentiating into fibroblasts (Vimetin-positive, GFAP-negative, Fig. S2). (F) Additionally, many cells expressed SMA (red) or AFP (yellow). Scale bar in F for A-E. (For interpretation of the references to colour in this figure legend, the reader is referred to the web version of this article.)

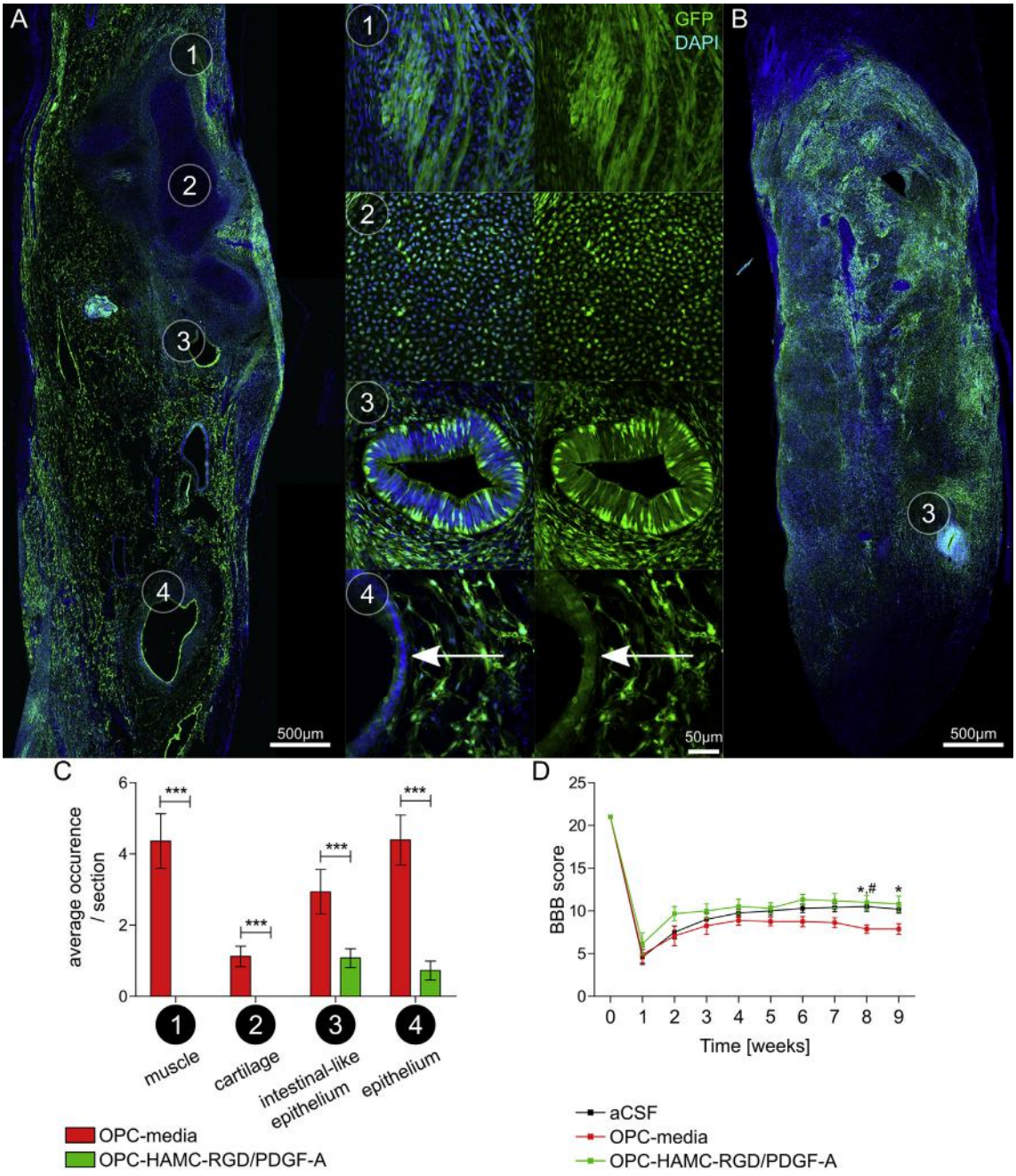

Fig. 7. HAMC-RGD/PDGF-A attenuates tumour formation. (A) Morphology and immunohistochemistry of spinal cord tissue suggests: (1) muscle, (2) cartilage, (3) intestinal-like epithelium, and (4) epithelium (arrow). (B) Limited number of epithelial structures are found in the OPC-HAMC-RGD/PDGF-A group. (C) Quantification of these structures demonstrates that the hydrogel attenuates teratoma formation of the remaining/undifferentiated iPS-derived transplanted cells. Only epithelial tissue is found in animals receiving OPCs in HAMC-RGD/PDGF-A. (D) BBB locomotor rating scale for animals receiving aCSF, OPC-media, or OPC-HAMC-RGD/PDGF-A. Data are plotted as mean ± SEM, n ≥ 8 sections/animal, $^{*,\#}p < 0.05$, $^{***}p < 0.001$ (* OPC-media vs. OPC-HAMC-RGD/PDGF-A, # OPC-media vs. aCSF). (For interpretation of the references to colour in this figure legend, the reader is referred to the web version of this article.)

the immune reaction. At 9 wpi, there was evidence of teratoma formation, which complicated the tissue analysis.

Cells transplanted in HAMC-RGD/PDGF-A were more morphologically homogenous and the majority of cells expressed markers associated with astrocytes (GFAP) or OPCs (SOX10) at 9 wpi, whereas cells transplanted in media appeared more heterogeneous and, while some cells still expressed SOX10, the majority de-differentiated into fibroblasts or differentiated into cells of mesodermal and endodermal origin. Although half of the animals in the OPC-HAMC-RGD/PDGF-A group also showed signs of tumor formation, this was not as extensive as that in the OPC-media group. The increased glial differentiation in the OPC-HAMC-RGD/PDGF-A group is probably due to the continued presentation of differentiation cues (PDGF-A and RGD), which was also shown to promote the differentiation of rodent NPCs *in vitro* [20]. While unmodified HAMC had no effect on oligodendroglial differentiation of rodent NPCs *in vitro*, HAMC-PDGF-A was sufficient to promote their differentiation into RIP-positive cells [20,24]. Interestingly, HAMC-PDGF-A did not promote the differentiation of grafted NPCs *in vivo* [24].

The ultimate goal in cell transplantation is tissue regeneration and functional repair. While several studies correlated improved functional recovery of animals receiving NPC to their differentiation into oligodendrocytes, recent studies in rodents demonstrated that newly generated host oligodendrocytes remyelinate spared axons [14,65]. Even in shiverer mice (which do not have endogenous myelin), only a small percentage of transplanted human iPS-derived OPCs contributed to the myelination of nude axons [12]. Similar to the shiverer mouse model, we found only a few cells that fully differentiated into mature oligodendrocytes and myelinated axons at the rim of the lesion.

Interestingly, after an initial phase of recovery similar to that observed for the aCSF control group, we observed a decline in motor function starting at 6 weeks. This is consistent with other studies, where unsafe mouse iPS-derived secondary neurospheres led to a decline in motor function 6 weeks after transplantation into an experimental mouse model of SCI [66]. Although HAMC-RGD/PDGF-A attenuated teratoma formation, this did not lead to an improvement in motor function over aCSF controls. This might be due to an insufficient number of cells that either differentiated into mature oligodendrocytes or integrated into the nervous system, or to the teratoma formation (albeit reduced) that was observed in this group. Animals that had OPCs injected in HAMC-RGD/PDGF-A had higher BBB scores at 8 and 9 weeks after injury compared to those animals that had OPCs injected in media, which likely reflects the decline in function of the latter due to teratoma formation. For a similar reason, animals that had simply aCSF injected showed better locomotor function than those with OPCs in media at 8 wpi.

Given that Wang et al. did not observe evidence of tumorigenesis from implanted hiPSC-derived OPCs at time points as long as 9 months after transplantation [12], we attribute the tendency of our OPCs to form teratomas to the shorter differentiation period. In Wang et al., the prolonged differentiation protocols may have effectively eliminated any residual undifferentiated cells prior to transplantation. Alternatively, the difference in teratoma formation may simply reflect the different cell lines and their respective potential for tumor formation [67]. Furthermore, a difference in tumor formation was observed between mouse embryonic stem cell-derived cells grown as spheres or as monolayers. Cells grown as spheres demonstrated tumor formation while adherent cells did not [68,69]. High-density culture conditions, as used for the OPCs after clonal generation from the neurospheres, has the potential to carryover teratoma-forming ES cells to the transplantable population [27]. Unfortunately, even a few undifferentiated cells, which are difficult to detect, can have a negative impact.

While HAMC-RGD/PDGF-A promoted the differentiation of transplanted OPCs *in vivo*, tumor formation was not completely eliminated and the presented data indicates that the either cell line or its culture as spheres is unsuitable for human use. Cell sorting of the OPCs prior to transplantation [70] or treating them with quercetin or YM155 may eliminate pluripotent cells and decrease the risk of tumorigenesis [9]. The strategy to combine sorting or chemical treatment of pluripotent stem cell-derived cultures with transplantation in peptide modified hydrogels might be one way to greatly reduce the potential of tumorigenesis in addition to influencing cell survival, integration and fate. Furthermore, the hydrogel used in this study degrades relatively quickly, with only ~3% of HA and ~20% of MC still present after 7 days [71,72]. We modified MC of HAMC due to its slower degradation time, and suggest that longer exposure to PDGF-A might have further reduced teratoma formation.

5. Conclusion

In conclusion, we demonstrate that the HAMC hydrogel, modified with a RGD peptide and PDGF-A, promoted early survival and integration of grafted cells. While the cells formed teratomas in all animals when injected in traditional media, only half of the animals had teratomas when cells were injected in HAMC-RGD/PDGF-A, demonstrating that the hydrogel attenuated tumour formation. This indicates that either the cells or their *in vitro* culture as spheres are unsuitable for human translation. Not only did we find fewer animals with teratomas when injected with OPCs in HAMC-RGD/PDGF-A, the ones that did have teratomas, had fewer structures with epithelial cellular characteristics, and no muscle or cartilage tissue. Most cells transplanted in the hydrogel differentiated to a glial phenotype. Thus, this hydrogel promoted cell survival and integration, and attenuated teratoma formation by promoting cell differentiation. Minimally invasive materials that can address transplantation barriers in a multifaceted approach, as shown here with peptide and growth factor modified HAMC, have great potential for future cell therapies. Further understanding the interplay of cell survival along with integration and differentiation signals can lead to new designs of clinically relevant strategies for treating CNS diseases for which no regenerative strategies currently exist.

Acknowledgments

We thank the Shoichet Lab for thoughtful review of this manuscript. We are grateful to Mrs. Rita van Bendegem for tissue processing, Mr. Peter Poon for animal surgery, Ms. Jill Harrop for assistance with immunohistochemistry and fluorescence imaging and Dr. Fehlings' lab for help with animal care. We thank the Canadian Institutes of Health Research (CIHR to MSS) and the Wings for Life Foundation for funding (to M.S.S.) and the CIHR TPRM training fellowship (to T.F.).

Appendix A. Supplementary data

Supplementary data related to this article can be found at http://dx.doi.org/10.1016/j.biomaterials.2015.12.032.

References

[1] W. Tetzlaff, E.B. Okon, S. Karimi-Abdolrezaee, C.E. Hill, J.S. Sparling, J.R. Plemel, et al., A systematic review of cellular transplantation therapies for spinal cord injury, J. Neurotrauma 28 (2011) 1611–1682, http://dx.doi.org/10.1089/neu.2009.1177.

[2] R.P. Salewski, R.A. Mitchell, L. Li, C. Shen, M. Milekovskaia, A. Nagy, et al., Transplantation of induced pluripotent stem cell-derived neural stem cells mediate functional recovery following thoracic spinal cord injury through remyelination of axons, Stem Cells Transl. Med. 4 (2015) 743–754, http://dx.doi.org/10.5966/sctm.2014-0236.

[3] K. Pfeifer, M. Vroemen, M. Caioni, L. Aigner, U. Bogdahn, N. Weidner, Autologous adult rodent neural progenitor cell transplantation represents a feasible strategy to promote structural repair in the chronically injured spinal cord, Regen. Med. 1 (2006) 255–266, http://dx.doi.org/10.2217/17460751.1.2.255.

[4] M. Schuldiner, J. Itskovitz-Eldor, N. Benvenisty, Selective ablation of human embryonic stem cells expressing a "suicide" gene, Stem Cells Dayt. Ohio 21 (2003) 257–265, http://dx.doi.org/10.1634/stemcells.21-3-257.

[5] Z. Rong, X. Fu, M. Wang, Y. Xu, A scalable approach to prevent teratoma formation of human embryonic stem cells, J. Biol. Chem. 287 (2012) 32338–32345, http://dx.doi.org/10.1074/jbc.M112.383810.

[6] S. Chung, B.-S. Shin, E. Hedlund, J. Pruszak, A. Ferree, U.J. Kang, et al., Genetic selection of sox1GFP-expressing neural precursors removes residual tumorigenic pluripotent stem cells and attenuates tumor formation after transplantation, J. Neurochem. 97 (2006) 1467–1480, http://dx.doi.org/10.1111/j.1471-4159.2006.03841.x.

[7] C. Tang, A.S. Lee, J.-P. Volkmer, D. Sahoo, D. Nag, A.R. Mosley, et al., An antibody against SSEA-5 glycan on human pluripotent stem cells enables removal of teratoma-forming cells, Nat. Biotechnol. 29 (2011) 829–834, http://dx.doi.org/10.1038/nbt.1947.

[8] A.B. Choo, H.L. Tan, S.N. Ang, W.J. Fong, A. Chin, J. Lo, et al., Selection against undifferentiated human embryonic stem cells by a cytotoxic antibody recognizing podocalyxin-like protein-1, Stem Cells Dayt. Ohio 26 (2008) 1454–1463, http://dx.doi.org/10.1634/stemcells.2007-0576.

[9] M.-O. Lee, S.H. Moon, H.-C. Jeong, J.-Y. Yi, T.-H. Lee, S.H. Shim, et al., Inhibition of pluripotent stem cell-derived teratoma formation by small molecules, Proc.

Natl. Acad. Sci. 110 (2013) E3281–E3290, http://dx.doi.org/10.1073/pnas.1303669110.
[10] O. Brustle, K.N. Jones, R.D. Learish, K. Karram, K. Choudhary, O.D. Wiestler, et al., Embryonic stem cell-derived glial precursors: a source of myelinating transplants, Science 285 (1999) 754–756.
[11] S.C. Zhang, B. Ge, I.D. Duncan, Adult brain retains the potential to generate oligodendroglial progenitors with extensive myelination capacity, Proc. Natl. Acad. Sci. U A 96 (1999) 4089–4094.
[12] S. Wang, J. Bates, X. Li, S. Schanz, D. Chandler-Militello, C. Levine, et al., Human iPSC-derived oligodendrocyte progenitor cells can myelinate and rescue a mouse model of congenital hypomyelination, Cell Stem Cell. 12 (2013) 252–264, http://dx.doi.org/10.1016/j.stem.2012.12.002.
[13] G.I. Nistor, M.O. Totoiu, N. Haque, M.K. Carpenter, H.S. Keirstead, Human embryonic stem cells differentiate into oligodendrocytes in high purity and myelinate after spinal cord transplantation, Glia 49 (2005) 385–396, http://dx.doi.org/10.1002/glia.20127.
[14] H.S. Keirstead, G. Nistor, G. Bernal, M. Totoiu, F. Cloutier, K. Sharp, et al., Human embryonic stem cell-derived oligodendrocyte progenitor cell transplants remyelinate and restore locomotion after spinal cord injury, J. Neurosci. 25 (2005) 4694–4705, http://dx.doi.org/10.1523/JNEUROSCI.0311-05.2005.
[15] C.T. Scott, D. Magnus, Wrongful termination: lessons from the geron clinical trial, Stem Cells Transl. Med. 3 (2014) 1398–1401, http://dx.doi.org/10.5966/sctm.2014-0147.
[16] M. Modo, R.P. Stroemer, E. Tang, S. Patel, H. Hodges, Effects of implantation site of dead stem cells in rats with stroke damage, Neuroreport 14 (2003) 39–42, http://dx.doi.org/10.1097/01.wnr.0000053066.88427.c2.
[17] A.J. Anderson, D.L. Haus, M.J. Hooshmand, H. Perez, C.J. Sontag, B.J. Cummings, Achieving stable human stem cell engraftment and survival in the CNS: is the future of regenerative medicine immunodeficient? Regen. Med. 6 (2011) 367–406, http://dx.doi.org/10.2217/rme.11.22.
[18] S. Sart, T. Ma, Y. Li, Preconditioning stem cells for in vivo delivery, BioRes. Open Access 3 (2014) 137–149, http://dx.doi.org/10.1089/biores.2014.0012.
[19] B.G. Ballios, M.J. Cooke, L. Donaldson, B.L.K. Coles, C.M. Morshead, D. van der Kooy, et al., A hyaluronan-based injectable hydrogel improves the survival and integration of stem cell progeny following transplantation, Stem Cell Rep. 4 (2015) 1031–1045, http://dx.doi.org/10.1016/j.stemcr.2015.04.008.
[20] R.Y. Tam, M.J. Cooke, M.S. Shoichet, A covalently modified hydrogel blend of hyaluronan-methyl cellulose with peptides and growth factors influences neural stem/progenitor cell fate, J. Mater. Chem. 22 (2012) 19402–19411, http://dx.doi.org/10.1039/C2jm33680d.
[21] A.E. Carson, T.H. Barker, Emerging concepts in engineering extracellular matrix variants for directing cell phenotype, Regen. Med. 4 (2009) 593–600, http://dx.doi.org/10.2217/rme.09.30.
[22] T.H. Barker, The role of ECM proteins and protein fragments in guiding cell behavior in regenerative medicine, Biomaterials 32 (2011) 4211–4214, http://dx.doi.org/10.1016/j.biomaterials.2011.02.027.
[23] S.L. Bellis, Advantages of RGD peptides for directing cell association with biomaterials, Biomaterials 32 (2011) 4205–4210.
[24] A.J. Mothe, R.Y. Tam, T. Zahir, C.H. Tator, M.S. Shoichet, Repair of the injured spinal cord by transplantation of neural stem cells in a hyaluronan-based hydrogel, Biomaterials 34 (2013) 3775–3783, http://dx.doi.org/10.1016/j.biomaterials.2013.02.002.
[25] K. Woltjen, I.P. Michael, P. Mohseni, R. Desai, M. Mileikovsky, R. Hamalainen, et al., piggyBac transposition reprograms fibroblasts to induced pluripotent stem cells, Nature 458 (2009) 766–770, http://dx.doi.org/10.1038/nature07863.
[26] B.Y. Hu, Z.W. Du, S.C. Zhang, Differentiation of human oligodendrocytes from pluripotent stem cells, Nat. Protoc. 4 (2009) 1614–1622, http://dx.doi.org/10.1038/nprot.2009.186.
[27] R. Chaddah, M. Arntfield, S. Runciman, L. Clarke, D. van der Kooy, Clonal neural stem cells from human embryonic stem cell colonies, J. Neurosci. 32 (2012) 7771–7781, http://dx.doi.org/10.1523/JNEUROSCI.3286-11.2012.
[28] V. Tropepe, S. Hitoshi, C. Sirard, T.W. Mak, J. Rossant, D. van der Kooy, Direct neural fate specification from embryonic stem cells: a primitive mammalian neural stem cell stage acquired through a default mechanism, Neuron 30 (2001) 65–78.
[29] S.R. Smukler, S.B. Runciman, S. Xu, D. van der Kooy, Embryonic stem cells assume a primitive neural stem cell fate in the absence of extrinsic influences, J. Cell Biol. 172 (2006) 79–90, http://dx.doi.org/10.1083/jcb.200508085.
[30] F.-P. Wachs, S. Couillard-Despres, M. Engelhardt, D. Wilhelm, S. Ploetz, M. Vroemen, et al., High efficacy of clonal growth and expansion of adult neural stem cells, Lab. Investig. J. Tech. Methods Pathol. 83 (2003) 949–962.
[31] L.Y. Chan, E.K.F. Yim, A.B.H. Choo, Normalized median fluorescence: an alternative flow cytometry analysis method for tracking human embryonic stem cell states during differentiation, Tissue Eng. Part C Methods 19 (2013) 156–165, http://dx.doi.org/10.1089/ten.TEC.2012.0150.
[32] I. Buchwalow, V. Samoilova, W. Boecker, M. Tiemann, Non-specific binding of antibodies in immunohistochemistry: fallacies and facts, Sci. Rep. 1 (2011) 28, http://dx.doi.org/10.1038/srep00028.
[33] G. Turaç, C.J. Hindley, R. Thomas, J.A. Davis, M. Deleidi, T. Gasser, et al., Combined flow cytometric analysis of surface and intracellular antigens reveals surface molecule markers of human neuropoiesis, PloS One 8 (2013) e68519, http://dx.doi.org/10.1371/journal.pone.0068519.
[34] W.S. Craig, S. Cheng, D.G. Mullen, J. Blevitt, M.D. Pierschbacher, Concept and progress in the development of RGD-containing peptide pharmaceuticals, Biopolymers 37 (1995) 157–175, http://dx.doi.org/10.1002/bip.360370209.
[35] Y. Aizawa, N. Leipzig, T. Zahir, M. Shoichet, The effect of immobilized platelet derived growth factor AA on neural stem/progenitor cell differentiation on cell-adhesive hydrogels, Biomaterials 29 (2008) 4676–4683, http://dx.doi.org/10.1016/j.biomaterials.2008.08.018.
[36] A.S. Rivlin, C.H. Tator, Effect of duration of acute spinal cord compression in a new acute cord injury model in the rat, Surg. Neurol. 10 (1978) 38–43.
[37] P.C. Poon, D. Gupta, M.S. Shoichet, C.H. Tator, Clip compression model is useful for thoracic spinal cord injuries: histologic and functional correlates, Spine Phila Pa 1976 (32) (2007) 2853–2859, http://dx.doi.org/10.1097/BRS.0b013e31815b7e6b.
[38] M.C. Jimenez Hamann, E.C. Tsai, C.H. Tator, M.S. Shoichet, Novel intrathecal delivery system for treatment of spinal cord injury, Exp. Neurol. 182 (2003) 300–309.
[39] A. Kawa, M. Stahlhut, A. Berezin, E. Bock, V. Berezin, A simple procedure for morphometric analysis of processes and growth cones of neurons in culture using parameters derived from the contour and convex hull of the object1, J. Neurosci. Methods 79 (1998) 53–64, http://dx.doi.org/10.1016/S0165-0270(97)00165-9.
[40] C. Yang, S. Przyborski, M.J. Cooke, X. Zhang, R. Stewart, G. Anyfantis, et al., A key role for telomerase reverse transcriptase unit in modulating human embryonic stem cell proliferation, cell cycle dynamics, and in vitro differentiation, Stem Cells 26 (2008) 850–863, http://dx.doi.org/10.1634/stemcells.2007-0677.
[41] D.M. Basso, M.S. Beattie, J.C. Bresnahan, A sensitive and reliable locomotor rating scale for open field testing in rats, J. Neurotrauma 12 (1995) 1–21.
[42] A. Hsieh, T. Zahir, Y. Lapitsky, B. Amsden, W. Wan, M.S. Shoichet, Hydrogel/electrospun fiber composites influence neural stem/progenitor cell fate, Soft Matter 6 (2010) 2227–2237, http://dx.doi.org/10.1039/b924349f.
[43] B.Y. Hu, Z.W. Du, X.J. Li, M. Ayala, S.C. Zhang, Human oligodendrocytes from embryonic stem cells: conserved SHH signaling networks and divergent FGF effects, Development 136 (2009) 1443–1452, http://dx.doi.org/10.1242/dev.029447.
[44] A.J. Crang, J. Gilson, W.F. Blakemore, The demonstration by transplantation of the very restricted remyelinating potential of post-mitotic oligodendrocytes, J. Neurocytol. 27 (1998) 541–553.
[45] J. Riley, T. Federici, J. Park, M. Suzuki, C.K. Franz, C. Tork, et al., Cervical spinal cord therapeutics delivery: preclinical safety validation of a stabilized microinjection platform, Neurosurgery 65 (2009) 754–761, http://dx.doi.org/10.1227/01.NEU.0000343524.45387.9E discussion 761–2.
[46] J.G. Weinger, B.M. Weist, W.C. Plaisted, S.M. Klaus, C.M. Walsh, T.E. Lane, MHC mismatch results in neural progenitor cell rejection following spinal cord transplantation in a model of viral-induced demyelination, Stem Cells 30 (2012) 2584–2595, http://dx.doi.org/10.1002/stem.1234.
[47] R. Dressel, J. Schindehütte, T. Kuhlmann, L. Elsner, P. Novota, P.C. Baier, et al., The tumorigenicity of mouse embryonic stem cells and in vitro differentiated neuronal cells is controlled by the recipients' immune response, PLoS One 3 (2008), http://dx.doi.org/10.1371/journal.pone.0002622.
[48] Y. Wang, M.J. Cooke, N. Sachewsky, C.M. Morshead, M.S. Shoichet, Bioengineered sequential growth factor delivery stimulates brain tissue regeneration after stroke, J. Control. Release Off. J. Control. Release Soc. 172 (2013) 1–11, http://dx.doi.org/10.1016/j.jconrel.2013.07.032.
[49] J.W. Austin, C.E. Kang, M.D. Baumann, L. DiDiodato, K. Satkunendrarajah, J.R. Wilson, et al., The effects of intrathecal injection of a hyaluronan-based hydrogel on inflammation, scarring and neurobehavioural outcomes in a rat model of severe spinal cord injury associated with arachnoiditis, Biomaterials 33 (2012) 4555–4564, http://dx.doi.org/10.1016/j.biomaterials.2012.03.022.
[50] T. Fuehrmann, J. Gerardo-Nava, G.A. Brook, Central Nervous System, in: Tissue Eng. Lab Clin, Springer-Verlag Berlin, Berlin, 2011, pp. 221–244.
[51] M. Janiszewska, C.D. Vito, M.-A.L. Bitoux, C. Fusco, I. Stamenkovic, Transportin regulates nuclear import of CD44, J. Biol. Chem. 285 (2010) 30548–30557, http://dx.doi.org/10.1074/jbc.M109.075838.
[52] H. Ponta, L. Sherman, P.A. Herrlich, CD44: From adhesion molecules to signalling regulators, Nat. Rev. Mol. Cell Biol. 4 (2003) 33–45, http://dx.doi.org/10.1038/nrm1004.
[53] M.W. Weible, T. Chan-Ling, Phenotypic characterization of neural stem cells from human fetal spinal cord: synergistic effect of LIF and BMP4 to generate astrocytes, Glia 55 (2007) 1156–1168, http://dx.doi.org/10.1002/glia.20539.
[54] Y. Liu, S.S.W. Han, Y. Wu, T.M.F. Tuohy, H. Xue, J. Cai, et al., CD44 expression identifies astrocyte-restricted precursor cells, Dev. Biol. 276 (2004) 31–46, http://dx.doi.org/10.1016/j.ydbio.2004.08.018.
[55] R.Y. Tam, T. Fuehrmann, N. Mitrousis, M.S. Shoichet, Regenerative therapies for central nervous system diseases: a biomaterials approach, Neuropsychopharmacol. Off. Publ. Am. Coll. Neuropsychopharmacol 39 (2014) 169–188, http://dx.doi.org/10.1038/npp.2013.237.
[56] S.M. Frisch, R.A. Screaton, Anoikis mechanisms, Curr. Opin. Cell Biol. 13 (2001) 555–562.
[57] M.J. Cooke, T. Zahir, S.R. Phillips, D.S. Shah, D. Athey, J.H. Lakey, et al., Neural differentiation regulated by biomimetic surfaces presenting motifs of extracellular matrix proteins, J. Biomed. Mater. Res. A 93 (2010) 824–832, http://dx.doi.org/10.1002/jbm.a.32585.
[58] Y. Luo, M.S. Shoichet, A photolabile hydrogel for guided three-dimensional cell growth and migration, Nat. Mater 3 (2004) 249–253.
[59] L.M. Yu, K. Kazazian, M.S. Shoichet, Peptide surface modification of methacrylamide chitosan for neural tissue engineering applications, J. Biomed.

Mater. Res. A 82 (2007) 243–255, http://dx.doi.org/10.1002/jbm.a.31069.
[60] T.I. Gudz, H. Komuro, W.B. Macklin, Glutamate stimulates oligodendrocyte progenitor migration mediated via an αv integrin/myelin proteolipid protein complex, J. Neurosci. 26 (2006) 2458–2466, http://dx.doi.org/10.1523/JNEUROSCI.4054-05.2006.
[61] J. Hu, L. Deng, X. Wang, X.-M. Xu, Effects of extracellular matrix molecules on the growth properties of oligodendrocyte progenitor cells in vitro, J. Neurosci. Res. 87 (2009) 2854–2862, http://dx.doi.org/10.1002/jnr.22111.
[62] V.E. Miron, A. Boyd, J.-W. Zhao, T.J. Yuen, J.M. Ruckh, J.L. Shadrach, et al., M2 microglia and macrophages drive oligodendrocyte differentiation during CNS remyelination, Nat. Neurosci. 16 (2013) 1211–1218, http://dx.doi.org/10.1038/nn.3469.
[63] J.C. Gensel, B. Zhang, Macrophage activation and its role in repair and pathology after spinal cord injury, Brain Res. 1619 (2015) 1–11, http://dx.doi.org/10.1016/j.brainres.2014.12.045.
[64] S. Vadivelu, T.J. Stewart, Y. Qu, K. Horn, S. Liu, Q. Li, et al., NG2+ progenitors derived from embryonic stem cells penetrate glial scar and promote axonal outgrowth into white matter after spinal cord injury, Stem Cells Transl. Med. 4 (2015) 401–411, http://dx.doi.org/10.5966/sctm.2014-0107.
[65] Z.C. Hesp, E.A. Goldstein, C.J. Miranda, B.K. Kaspar, D.M. McTigue, Chronic Oligodendrogenesis and remyelination after spinal cord injury in mice and rats, J. Neurosci. 35 (2015) 1274–1290, http://dx.doi.org/10.1523/JNEUROSCI.2568-14.2015.
[66] S. Nori, Y. Okada, A. Yasuda, O. Tsuji, Y. Takahashi, Y. Kobayashi, et al., Grafted human-induced pluripotent stem-cell-derived neurospheres promote motor functional recovery after spinal cord injury in mice, Proc. Natl. Acad. Sci. U. S. A. 108 (2011) 16825–16830.
[67] M. Nakamura, H. Okano, Cell transplantation therapies for spinal cord injury focusing on induced pluripotent stem cells, Cell Res. 23 (2013) 70–80, http://dx.doi.org/10.1038/cr.2012.171.
[68] Y. Guan, Q.-A. Du, W. Zhu, C. Zou, D. Wu, L. Chen, et al., Function of mouse embryonic stem cell-derived supporting cells in neural progenitor cell maturation and long term cxpansion, PLoS One 8 (2013), http://dx.doi.org/10.1371/journal.pone.0054332.
[69] Q. an Du, Y. Guan, H. Ji, Z. Chen, Y.A. Zhang, Effect of monolayer cells on sphere cells–two types of cells that emerge during the neural differentiation of mouse embryonic stem cells, Neurosci. Lett. 504 (2011) 285–289, http://dx.doi.org/10.1016/j.neulet.2011.09.048.
[70] F.J. Sim, C.R. McClain, S.J. Schanz, T.L. Protack, M.S. Windrem, S.A. Goldman, CD140a identifies a population of highly myelinogenic, migration-competent and efficiently engrafting human oligodendrocyte progenitor cells, Nat. Biotechnol. 29 (2011) 934–941, http://dx.doi.org/10.1038/nbt.1972.
[71] B.G. Ballios, M.J. Cooke, D. van der Kooy, M.S. Shoichet, A hydrogel-based stem cell delivery system to treat retinal degenerative diseases, Biomaterials 31 (2010) 2555–2564, http://dx.doi.org/10.1016/j.biomaterials.2009.12.004.
[72] C.E. Kang, P.C. Poon, C.H. Tator, M.S. Shoichet, A new paradigm for local and sustained release of therapeutic molecules to the injured spinal cord for neuroprotection and tissue repair, Tissue Eng. Part A 15 (2009) 595–604, http://dx.doi.org/10.1089/ten.tea.2007.0349.